

## Mathematical Modelling of Nonlinear Characteristics of RC Plates and Shells

T. TANABE, Z. S. WU

*Nagoya University, Nagoya, Japan*

T. UTSUNOMIYA

*Shikoku Electric Power Co., Inc., Nishiwagun, Japan*

G. HIROSE

*Shikoku Electric Power Co., Inc., Takamatsu, Japan*

## ABSTRACT

The unified constitutive equation which considers the coupled effects of tension stiffening and concrete-to-concrete friction of a reinforced concrete element has been derived. Numerical analysis was compared with the experimental results. Based on these results, the finite displacement analysis has been performed for a RC beam, wall and plate with stability consideration. On these results, the failure mechanism of the structures was discussed.

## 1 INTRODUCTION

Application of the finite element method to the analysis of a reinforced concrete member or a structure has advanced substantially to the present moment. However, it soon encounters difficulty when the structure meets the occurrence of multiple crackings. In other words, if the crack occurs to three different orientations, the usual FEM code cannot cope with it. The present formulation is specially aimed for those situations and some applications will be treated in the paper. In the second phase of the study, the same formulation, though much simplified, will be applied to the study of failure mechanism of RC structures.

Failure of the structures is known to be affected by tension stiffness, shear transfer, cracking pattern, strength of intact concrete, bond-slip relation of tensile reinforcement, and so on. Those factors, combined altogether with the configuration of the member, give rise to the total failure phenomena. The complicated failure mechanism leads to diversity of different failure modes. One way of enabling theoretical insight into this diversity of failure phenomena will be the adoption of the eigen mode analysis at each critical point with thorough covering of the secondary effect of the displacement.

## 2 CONSTITUTIVE LAWS OF CRACKED RC ELEMENTS FOR MIXED MODE

For the cracked reinforced concrete element, the shear forces and normal forces are supposed to be applied. Taking out a representative portion between two cracks as shown in Fig.1a, it is possible to separate the concrete into two regions, one in which compressive force is working to the normal direction for crack surfaces and the other region where tensile stress is working to the normal direction for cracked surfaces as shown in Fig.1b. The distribution of the concrete stresses between two adjacent cracks is derived as[1]

$$\sigma_{c,x} = \frac{\sigma_x}{(1 + np_x)} + \left( \frac{np_x \sigma_x}{1 + np_x} - \sigma_{s,x0} \right) \frac{\cosh(x/b_{cx})}{\cosh(\ell_{cx}/b_{cx})} \quad (1)$$

$$\sigma_{c,y} = \frac{\sigma_y}{(1 + np_y)} + \left( \frac{np_y \sigma_y}{1 + np_y} - \sigma_{s,y0} \right) \frac{\cosh(y/b_{cy})}{\cosh(\ell_{cy}/b_{cy})} \quad (2)$$

$$\sigma_{c,xy} = \tau_{x,y} \quad (3)$$

where the notations  $\ell_c$  and  $b_c$  with suffix  $x, y$  denote the crack spacings and the bond characteristics coefficients in the  $x$  and  $y$  directions, respectively,  $n$  is a ratio of Young's modulus of steel to that of concrete, and  $\sigma_{s,x0}$  and  $\sigma_{s,y0}$  are the stresses in the orthogonal reinforcement at the crack, respectively.

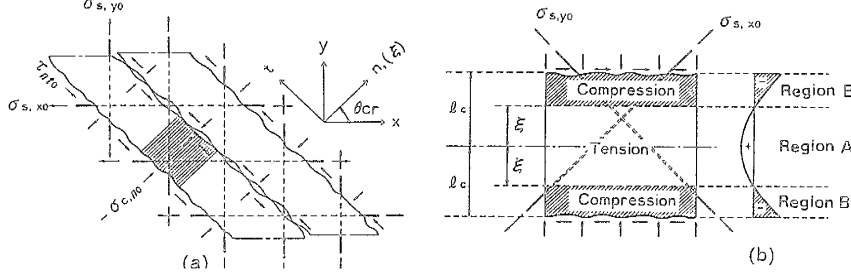


Fig.1 Stress Condition at A Crack in The Mixed Mode Displacement Condition

By considering the equilibrium equations of the free body, we have

$$\sigma_{s,x0} = \sigma_x + \sigma_{c,n0} + (\tau_{xy} + \tau_{nt0}) \tan \theta_{cr}, \quad \sigma_{s,y0} = \sigma_y + \sigma_{c,n0} + (\tau_{xy} - \tau_{nt0}) \cot \theta_{cr} \quad (4)$$

where  $\sigma_{c,n0}$  is the normal stress of concrete and  $\tau_{nt0}$  is the shear stress which is the sum of the shear resistance  $\tau_{c,nt0}$  due to aggregate interlocking and the shear resistance  $\tau_{d,nt0}$  due to the dowel action of reinforcement on the crack plane.

The location where concrete stress changes from compression to tension should satisfy the following equation.

$$\begin{aligned} c^2 \left( \sigma_{s,x0} - \frac{np_x \sigma_x}{1 + np_x} \right) \frac{\cosh(\xi / (b_{cx} c))}{\cosh(\ell_{cx} / b_{cx})} + s^2 \left( \sigma_{s,y0} - \frac{np_y \sigma_y}{1 + np_y} \right) \frac{\cosh(\xi / (b_{cy} s))}{\cosh(\ell_{cy} / b_{cy})} \\ = \frac{c^2 \sigma_x}{1 + np_x} + \frac{s^2 \sigma_y}{1 + np_y} + 2sc \tau_{xy} \end{aligned} \quad (5)$$

where  $c$  and  $s$  denote  $\cos \theta_{cr}$  and  $\sin \theta_{cr}$ , respectively. If  $\xi \leq 0$ , there exists no tension zone. However, if  $0 < \xi < \ell_c$  the stress state of an element in both compression and tension. Moreover, if  $\xi \geq \ell_c$  the stress state is in tension only, and there exists no shear slip on the crack plane. The portion where concrete is stressed in tension to the  $\xi$  direction, has to be treated as having slip between steel and concrete and its situation is exactly the same as the case of the S-mode (Separation mode)[1]. We separate the concrete portion along the  $\xi$  direction to the region B where  $\sigma_{c,n}$  is in compression and, to the regions A where  $\sigma_{c,n}$  is in tension. The concrete stress is zero at the boundary between A and B. Hence it can be considered that the constitutive equation which predicts the tension stiffness is applicable in the region A. For the region B, the stress and displacement field is mainly influenced by aggregate interlocking and the dowel action on the crack plane and the tension stiffening effect never occurs because the plane stress field of concrete is stressed in compression so that the constitutive equations developed for the F-mode (Frictional contact mode)[1] are considered to be applicable. However, the slipping out of a bar at the region A contributes to the crack opening of the region B, the total crack opening  $\delta_n$  and the total crack slip  $\delta_t$  should be the sum of the contributions from the region A and from the region B. Based on these considerations, we develop the constitutive equations for the mixed mode. Obviously, at the boundary of two regions, the stress equilibrium should be satisfied and also the stresses at the boundary of two regions should correspond to the applied stresses. Hence  $\{\sigma\}_A = \{\sigma\}_B = \{\sigma\}$ , and the total elongation of the portion between two cracks is the sum of the elongation of each region of A and B, and the total average strain  $\{\epsilon\}$  is written as

$$\begin{Bmatrix} \epsilon_n \\ \epsilon_t \\ \gamma_{nt} \end{Bmatrix} = \begin{bmatrix} \eta & 0 & 0 \\ 0 & \eta & 0 \\ 0 & 0 & \eta \end{bmatrix} \begin{Bmatrix} \epsilon_n \\ \epsilon_t \\ \gamma_{nt} \end{Bmatrix}_A + \begin{bmatrix} 1 - \eta & 0 & 0 \\ 0 & 1 - \eta & 0 \\ 0 & 0 & 1 - \eta \end{bmatrix} \begin{Bmatrix} \epsilon_n \\ \epsilon_t \\ \gamma_{nt} \end{Bmatrix}_B \quad (6)$$

where  $\eta$  is the fraction to the crack spacing of the length of the area where the concrete is in compression along the  $\xi$  direction and frictionless mode is predominant. This is written in the linear case as  $\eta = \xi/\ell_c$ . For multiple crack systems, the average values of  $\xi$  and  $\ell_c$  to each crack of different orientation are adopted. At this stage, it should be recalled that the constitutive equation for the S-mode is written as

$$\{\sigma\} = ([I] - [\Omega]_S) [D]_c \{\varepsilon\} \quad (7)$$

and for the F-mode, the similar equation is written as

$$\{\sigma\} = ([I] - [\Omega]_F) [D]_c \{\varepsilon\} \quad (8)$$

where  $[\Omega]_S$  and  $[\Omega]_F$  denote the stress reduction tensors in the S-mode and in the F-mode respectively. The detailed discussion on these tensors will be found in the ref.[1]. As we already have Eqs. (7) and (8) for the regions A and B, Eq.(6) is rewritten as

$$\{\sigma\} = ([I] - [\Omega]) [D]_c \{\varepsilon\}, \quad \{\Omega\} = [I] - \left( [\eta]([I] - [\Omega]_S)^{-1} + [\zeta]([I] - [\Omega]_F)^{-1} \right)^{-1} \quad (9)$$

Experiments corresponding to the mixed mode are very scarce, due to its complexity. However, Millard and Johnson [2] carried out this type of experiment using the specimen shown in Fig.2(a). They introduced a crack at the center of a specimen by applying tensile forces at both ends. Maintaining the tensile stress, the shear force was applied at the center. The stress condition of concrete is such that the compressive stress is working at the crack to the normal direction to a crack surfaces while the tensile force is working at the ends to the same direction. The experimental relations between the shear stress and the shear displacement are shown in comparison with the calculated relations in Figs.2(b),(c) (specimen mark: 2-5-8). In the calculation procedure, it is found that the shear rigidity is very dependent on the extent of fraction A.

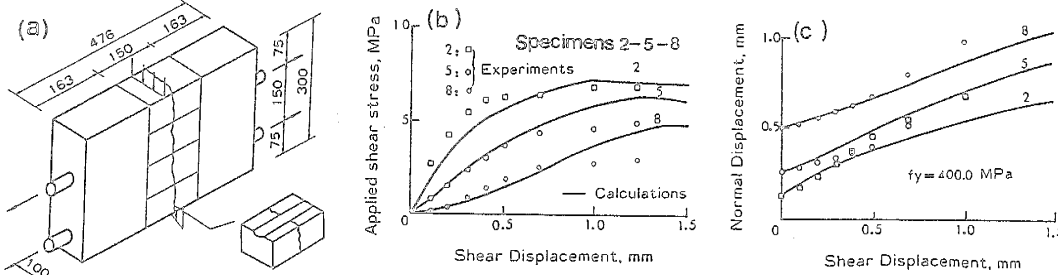


Fig.2 Prediction of Millard and Johnson's Experiment(1985)

### 3 FINITE DISPLACEMENT FORMULATION AND STABILITY ANALYSIS

The application of virtual work to the system will yield

$$\iiint (\sigma_{ij}^{(0)} + \sigma_{ij}) \delta (e_{ij}^{(0)} + e_{ij}) dV - \iiint (f_i^{(0)} + f_i) \delta (u_i^{(0)} + u_i) dS = 0 \quad (10)$$

where the summation convention rule is used and body force is neglected. The super subscript (0) denote the condition functions at  $i$ th step and the quantities without super script denote the incremental quantities in the  $(i + 1)$ th step. With proper use of displacement function and rewriting in the Cartesian Coordinate System, Eq.(10) will be reduced to the incremental form of

$$[K + K_0 + K_g]^{(n+1)} \{\Delta d\} = \{\Delta F\}^{(n+1)} + \{F_r\}^n \quad (11)$$

where  $[K]$  denotes the incremental stiffness matrix,  $[K_0]$  denotes the incremental initial strain matrix and  $[K_g]$  denotes the incremental geometrical stiffness matrix. The vector  $\{F_n\}$  denotes the unbalanced force vector at the  $n$ th step calculation and should be added at the  $(n + 1)$ th step and the vector  $\{\Delta d\}$  denotes incremental displacement vector.

An incremental iterative technique is adopted to solve the nonlinear equations. In order to trace the post-limit behaviour of the structures, the arc-length solution technique or displacement incrementation with the Newton-Raphson method has been implemented for the present study. As a convergence criterion for the iteration process, the residual force convergence criteria is used. (specified convergence tolerance =  $10^{-3}$ )

At each critical point, stability analysis has been performed[3]. Supposing that the lowest eigenvalue  $\lambda_1 = 0$  at the first critical point without loss of generality, then

$$\mu[V_1]^T\{F\} = 0 \quad (12)$$

where  $\mu$ ,  $F$  and  $[V_1]$  express load parameter, load vector and eigen mode corresponding to  $\lambda_1$ , respectively. In Eq.(12),  $\mu = 0$  denotes the limit point and  $[V_1]^T\{F\} = 0$  denotes the bifurcation point. The displacement in these critical point is given in the following. At the limit point it is self evident that

$$\Delta d = A * [V_1] \quad (13)$$

At the bifurcation point, we consider that

$$\Delta d = \alpha\{\Delta d\}^* + \beta\{V_1\} \quad (14)$$

where  $\alpha$  and  $\beta$  are the arbitrary constants as far as the total tangential stiffness matrix  $K^*$  remain constant and  $\{\Delta d\}^*$  denotes the particular displacement solution by reducing the rank of  $K^*$ . Since any small increase of displacement will change the  $K^*$  matrix,  $\alpha$  and  $\beta$  converges to certain values. In these ways, it is possible to find out the bifurcation point, as well as their mode of displacement. Especially, at the limit point, the displacement vector agrees with the eigen vector and it is considered that the first eigen vector strongly suggests the failure mode. At the bifurcation point, the linear combination of the fundamental mode and the first eigen vector suggest the failure mode.

#### 4 SOME MECHANICAL CONSIDERATION FOR FAILURE MODES

To investigate the failure mechanism of RC structures, three examples are analyzed in detail. One example is the deep beam the dimension of which is shown in Fig.3(a)[4]. The load and the displacement at the bottom relation is shown in Fig.3(c). The crack pattern at the ultimate strength stage is shown in Fig.3(b). The crack pattern together with the information of shear span to beam depth ratio of 1.3 suggested that the specimen failed in the shear compression failure mode.

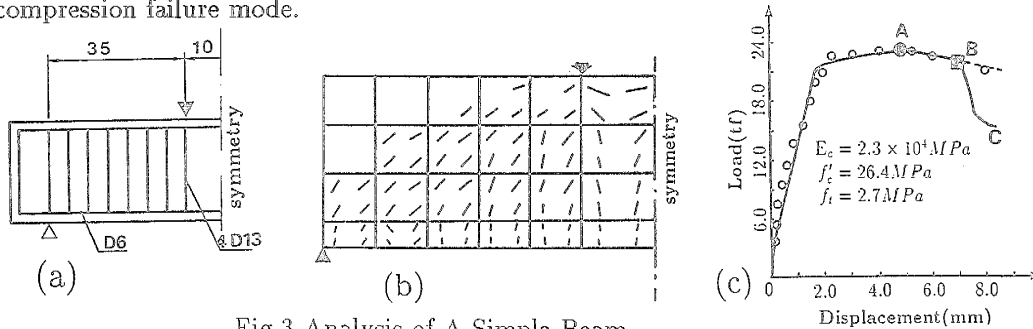


Fig.3 Analysis of A Simple Beam

The analysis showed that the shear failure was due to the bifurcation. As noticed in Fig.3(c), the total tangential stiffness matrix yields the negative eigenvalues at the point A. However, the eigen mode is almost the same in comparison with the previous step as shown in Figs.4(a),(b), and it is changed continuously around this point. It is considered that this

point should corresponds to the limit state of the structure. From the point, the structure is going into softening range in a state of unstable equilibrium, as expected. The eigen mode is kept unchanged until the new negative eigenvalues appears. However in point B, the third and the fourth eigenvalues become negative and the first and the second eigen modes are completely different from any eigen mode occurred previously as shown in Fig.4(c). Moreover, the dot product of load vector and the first or the second eigen mode vanishes approximately. Because of these considerations, the point B would correspond to the bifurcation point of the structure, where both the load and the deformation become unstable. After the bifurcation point B, the dashed lines is considered as the fundamental equilibrium path due to the continuous change of incremental deformation around the point B. Furthermore, with the investigation for the bifurcation path, another equilibrium path BC shown in Fig.3(c) can be obtained analytically. Here, the first eigen mode is considered as the initial displacement vector of the beam for the iteration. Along this path, the load capacity falls rapidly up to the collapse of the beam. The behavior until the final failure of the beam may be explained with the fact that the load-displacement relation is exactly on this path.

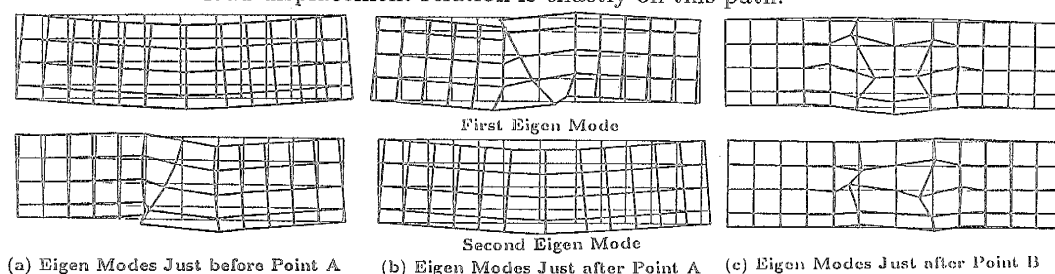


Fig.4 Eigen Modes at Some Critical Points

The second example treated here is the shear wall dimension of which is shown in Fig.5(a)[5]. The proposed constitutive equation of membrane element is directly adopted. The relations between the horizontal load and the horizontal displacement of the loaded point are shown in Fig.5(d). The numerical results again trace the maximum point and the softening behaviour of the structure. The stability analysis in this case showed that the eigen mode had continuous change from one step to the next around the maximum point and there is a strong indication that the maximum point be the limit point. The eigen mode just before and right after the the limit point was shown in Figs.5(e) and (f). The heavy damage seems to be existing at around the loaded point. However, the bifurcation seems not existing and rather smooth transition is observed from the initial loading to the maximum point and to softening region.

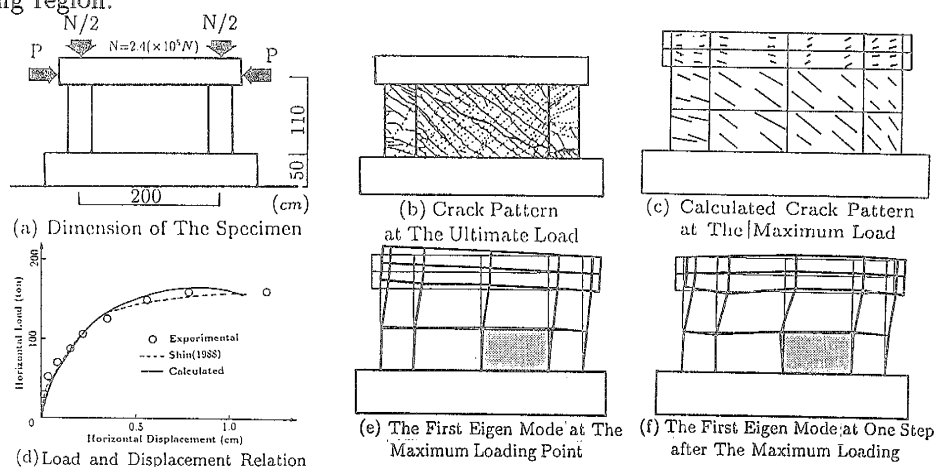


Fig.5 The Shear Wall Calculated

The last example is Taylor's two-way simply-supported slab to test the capability of the proposed model in plate bending application[6]. The employed material properties are simi-

lar to those used in ref.[7]. Details of the slab can be found in refs.[1],[6]. Comparison of the computed and the experimental response of load-deflection and collapse loads are shown in Fig.6 comparing with both Berg and Rajagopal's solutions. In their solutions, the deflections were overestimated as shown in the figure. It is easily found that at the increment where the first crack is developed, an increase in deflection values of about 600% over the value at the start of the increment took place. The overestimation of deflections of slabs in the intermediate ranges of loading appears to be a major problem. The main source of error is considered to be due to the lack of inadequate constitutive law of cracked elements which expresses rationally various kinds of nonlinearities, such as tension stiffening effect due to the occurrence of multiple cracking. Some success by adopting the proposed model can be found in the figure. With the proposed model, it is possible to allow an arbitrary number of cracks in an integration point. The cracking pattern as shown in Fig.7 at calculated ultimate load along the diagonals agrees with the diagonal yield line pattern during the actual slab experiment. The cracking of top layers near the corners due to corner uplift is also shown in the figure. In this example, the stability analysis has also carried out to investigate the behaviour of the maximum point which is really a limit point and no numerical difficulties were met to trace the post-limit behaviour.

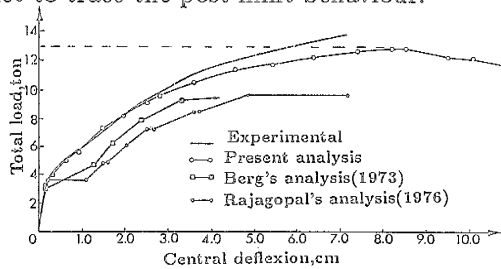


Fig.6 Load-Deflection Diagram for Taylor's Slab

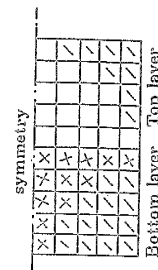


Fig.7 Cracking Pattern

## 6 CONCLUSION

The detailed constitutive equation to treat the cracked reinforced concrete element was derived based on the mixed mode deformation analysis. It is found that the model can predict the behavior of the element cracked to multiple directions. To study the failure mechanism of structures, then, the finite displacement formulation which includes stability analysis was developed. From the analysis of three simple examples, the shear failure is considered to be due to the instability of the system in some cases. Numerical simulations show that the consideration of nonlinear geometric behaviour may be indispensable to obtain a correct structural response, collapse load and failure mode, even for relatively small deflections.

## REFERENCES

- [1] Z.S. Wu, Development of Computational Models for Reinforced Concrete Plate and Shell Elements, Doctoral Dissertation presented to Nagoya University, March, 1990.
- [2] Millard, S.G. and Johnson, R.P., Shear Transfer in Cracked Reinforced Concrete, Magazine of Concrete Research, Vol.37, No.130, 3-15, 1985.
- [3] Tanabe, T., Z.S. Wu and Nakamura, H., Mixed Mode Formulation for Membrane Displacement Analysis of RC Plate and Shell Elements, Proc. Int. Workshop on Concrete Shear in Earthquake, Univ. of Houston, 1991.
- [4] S. Ikeda and H. Nagumo, Study on a Method of Rational Application of Finite Element Method to RC and PC Structures, Proc. of JSCE, No.414, V-12, pp.137-144, 1990.
- [5] Shin, H. M. Finite Element Analysis of RC Members Subjected to Reversed Cyclic In-plane Loadings, Doctoral Dissertation presented to Tokyo University, June, 1988.
- [6] Taylor, R. et al., Effect of the Arrangement of Reinforcement on the Behavior of Reinforced Concrete Slabs, Magazine of Concrete Research, Vol.18, No.55, 85-94, 1966.
- [7] Berg, S., Nonlinear Finite Element Analysis of Reinforced Concrete Plates, Proc. Second Int. Conf. on Struct. Mech. in Reactor Tech., Vol. M., Berlin, Germany, 1973.
- [8] Rajagopal, K., Nonlinear Analysis of RC Beams, Beam-Columns and Slabs by Finite Elements, Published on Demand by University Microfilms Int., England, 1976.